ISSN NO. 2320-5407

Journal homepage: http://www.journalijar.com

INTERNATIONAL JOURNAL OF ADVANCED RESEARCH

RESEARCH ARTICLE

Spectrophotometric Investigations of Some Thiazole-azo Dyes

Ritu Payal*

Department of Chemistry, University of Delhi, Delhi-110007, India

Manuscript Info

Manuscript History:

Received: 15 October 2015
Final Accepted: 26 November 2015
Published Online: December 2015

Key words:

Thiazole-azo dyes, absorption, antioxidant activity, free-radical, DPPH, Kamlet-Taft parameters, prototropic equilibria

Corresponding Author

Ritu Payal

Abstract

A series of thiazole-azo dyes i.e. 5-(phenyldiazenyl)-4-phenylthiazol-2-amines (PDTA) have been synthesized from their analogous coupling components. The absorption data of PDTA derivatives have been recorded in a series of solvents of varying polarity. They behave quite differently owing to solvent and substituent effects. The absorption spectra of these PDTA derivatives display an interesting unique behavior in DMSO. Kamlet-Taft and Catalán parameters have been used to describe the solvent effects and the absorption spectral shifts of the PDTA derivatives. These derivatives have been also screened for their *in vitro* antioxidant properties using 1,1-diphenyl-2-picrylhydrazyl free radical scavenging assay *via* ethanolic extracts of the dyes. The antioxidant strength of PDTA derivatives have been compared with the standard ascorbic acid and showed potent antioxidant activity. The absorption spectral characteristics of PDTA derivatives have been also investigated as a function of acidity and basicity (H_o/pH/H_) in aqueous phase and have been found to show azonium-ammonium tautomerism.

INTRODUCTION

The physical properties of azo dyes depend primarily on the size and substitution of the aromatic rings present in their structure. The azo dyes bearing five-membered heterocyclic thiazole ring have significant use in industry as disperse dyes (Geng *et al*., 2015; Wang *et al.*, 2012; Kaupp *et al*. 2004) and optical data storage devices (Åstrand *et al.*, 2000). In addition they have been reported to possess electrochemical (Nica *et al.*, 2011), photochromic and nonlinear optical properties (Raposo *et al.*, 2011). These dyes have also been found to show antimicrobial activity (Karci *et al*., 2009).

Along with different biological activities, azo dyes may exhibit interesting spectral behavior which are strongly influenced by the solvent and can be understood by investigation of solute-solvent interactions. The solvent effects are associated with the nature and the extent of the solute-solvent interactions developed locally within immediate vicinity of solute due to their strong dependence on the solvent polarity (Rastogi *et al.*, 2012, 2007, 2003, 2001a, 2001b). To further understand the spectral behavior as well various bonding interactions, a five-membered heterocyclic rings based thiazole-azo dyes (PDTA derivatives) have been synthesized.

Many derivatives containing five-membered ring have found to possess antioxidant activities (Osman *et al.*, 2012; Hassan 2012; Ishihara and Fujisawa, 2007), which enlightens to screen PDTA derivatives for their *in vitro* antioxidant properties using 1,1-diphenyl-2-picrylhydrazyl (DPPH$^{\bullet}$) free radical scavenging assay *via* ethanolic extracts of the PDTA derivatives using ascorbic acid as a standard reference.

Antioxidant functioning in biological systems is very much dependent on the chemistry of reactive oxygen species (ROS) such as hydroxyl radicals ($^{\bullet}OH$), superoxide radicals ($O_2^{\bullet-}$), singlet oxygen ($^1O_2$), hydrogen peroxide radical (H_2O_2). ROS results in ageing, atherosclerosis, heart disease, cancer, inflammation (rheumatoid arthritis, hypoxia-reperfusion injury, pancreatitis etc.), tissue damage, cell death *etc.* and are constantly formed as a result of

normal organ functions or excessive oxidative stress (Rawat *et al.*, 2012; Scott, 1997). These are regulated by interaction of complex antioxidant machineries and thereby, minimizing the adverse effects of free radicals in living systems. Compounds with amino group exhibit antimicrobial and antioxidant properties, since; they act as free radical scavengers due to presence of various substituents as well as extent of structure conjugation (Osman *et al.*, 2012; Devasagayam *et al.*, 2008).

DPPH˙ is a well-known stable free radical which acts as widely accepted tool in estimating free radical-scavenging activities of other radicals. It shows a deep violet color in solution, which exhibits a strong absorption band (λ_{max}) at 517 nm, and it appears colorless or pale yellow when neutralized. This property allows visual monitoring of the reaction and helps in measuring the continual decrease in absorbance of the DPPH˙ solution at 517 nm, in the presence of antioxidant compound. DPPH˙ contains odd electron at one atom of nitrogen bridge, it becomes paired in the presence of antioxidant due to transfer of proton from antioxidant and results in the decrease in its absorbance. Consequently, reduction in the rate of a chemical reaction upon addition of DPPH˙ indicates the radical nature of that reaction (Lin *et al.*, 2008).

In the present work, absorption spectral properties of PDTA derivatives have been studied in various solvents. The solvent effects on the absorption bands have been complemented using Kamlet-Taft and Catalán parameters. The antioxidant activity of the ethanolic extract of PDTA derivatives has been evaluated *in vitro* by the DPPH radical scavenging assay using spectrophotometric analysis. The analysis also involves their absorption spectral characteristics as a function of acidity and basicity (H_o/pH/H_) in aqueous phase.

2. Materials and Methods

2.1. *Chemicals*

All the required chemicals for the synthesis of PDTA derivatives were purchased from Spectrochem Pvt. Ltd. The solvents used to record absorption data (n-hexane, cyclohexane, DCM, DMF, acetonitrile, methanol etc.) were of spectroscopic grade and were checked for the absence of spectral impurities within requisite scanning range. DPPH and ascorbic acid used in the antioxidant activity was purchased from Spectrochem Pvt. Ltd. Analytical grade sulfuric acid, hydrochloric acid and sodium hydroxide were purchased from Rankem, S.D. Fine, India and BDH, India, respectively.

2.2. *Instrumentation*

The spectrophotometric data of PDTA derivatives were measured using an ANALYTIKA JENA UV WINASPECT SPECTROD PC 250 Spectrophotometer with 1 cm quartz cells at room temperature. 0.01 M stock solutions of PDTA derivatives were prepared by dissolving an accurate amount of the compound in requisite volume of the solvent. The stock solutions were diluted to 1×10^{-5} M to record their absorption spectra with matching quartz cuvettes.

The stock solution of standard ascorbic acid under consideration was prepared by dissolving 5 mg of the required compound in 50 ml ethanol. DPPH˙ stock solution was prepared by dissolving 4 mg in 50 ml in ethanol. The different concentration solutions (1000, 500, 250, 100, 50, 25 and 10 µg/ml) of different PDTA derivatives were prepared from the stock solution using suitable dilution. For pH studies, millipore water was used to prepare acidic and basic solutions. HCl-H_2O mixture and NaOH-H_2O mixture were used to prepare pH solutions from pH 1-14 and H_2SO_4-H_2O mixture was used for solutions below pH 1 according to Hammett's acidity scale (H_o) (Paul and Long, 1957). The pH values in the range of 1−14 were measured on Eutech's cyberscan pH meter, which was standardized at room temperature using standard buffers of pH 4, 7 and 9.

The purity of PDTA derivatives was checked by TLC, IR and ^{1}H NMR. Their melting points were determined using Buchi Melting Point M-560 apparatus.

2.3. *Determination of the DPPH Scavenging Activity*

DPPH free radical scavenging assay was carried out according to the following procedure (Berset *et al*., 1995). 1 ml of ethanolic solution of DPPH˙ was added to 1 ml of ethanolic extract of standard compound (ascorbic acid) and was used as control. Similarly, solution mixtures of different concentrations (1000, 500, 250, 100, 50, 25 and 10 µg/ml) were prepared, kept in dark for 30 minutes and their absorbance was measured at 517 nm. The % inhibitor activity was measured as a decrease in the absorbance of DPPH and was calculated using the following equation (eq.1):

$$\%\ \text{Inhibitor Activity} = \frac{(\text{Absorbance of control} - \text{Absorbance of sample})}{\text{Absorbance of control}} \times 100 \quad (1)$$

The tests were done in triplicate. The concentration of sample required to scavenge 50% of DPPH (IC_{50}) were determined. The IC_{50} values were calculated by linear regression of plots, where the abscissa represents the concentration of the tested compounds and the ordinate represents average percent of scavenging capacity.

2.4. *Synthesis of PDTA derivatives*

PDTA derivatives were synthesized using 4-phenylthiazole-2-amine as a starting material by following the procedure described in the literature (Bingol and Coskun, 2011; Kaupp *et al*. 2004) and their purity was confirmed by TLC, FT-IR, ^{1}H NMR and ^{13}C NMR.

2.4.1. 4-phenylthiazol-2-amine: A mixture of phenacyl bromide (0.1 M) and thiourea (0.1 M) in 10-15 ml of ethyl alcohol was refluxed in an oil bath for 5 hours at 70 °C. The progress of the reaction was monitored by TLC using 30% ethyl acetate and 70% petroleum ether solvent system. After cooling for half an hour at the room temperature, the reaction mixture was poured over crushed ice with vigorous stirring. The white precipitate thus obtained was washed with cold water to remove impurities. After drying, the compound was recrystallized using ethanol.

2.4.2. 5-(phenyldiazenyl)-4-phenyl thiazol-2-amine (H-PDTA)

(i) ***Preparation of diazonium salt:*** A solution of aniline (0.01 M) in 3 ml HCl (6 M) was allowed to cool for 2 hours in an ice-bath. The solution was stirred vigorously for 30-35 minutes. An ice cooled aqueous solution of sodium nitrite (0.7 g in 10 ml) was added drop wise to the reaction mixture with continuous stirring. The mixture was stirred for 40–45 minutes to obtain the diazonium salt solution to be used in coupling reaction.

(ii) ***Synthesis of H-PDTA:*** The diazonium salt solution prepared previously was added in lots to a well cooled solution of 4-phenylthiazol-2-amine (0.01 M) in ethanol (20 ml) and sodium acetate (4 g) with vigorous stirring. The reaction mixture was allowed to stir until the precipitate began to settle. During the course of reaction the temperature was maintained between 0–5 °C and pH was constrained to 4–6. The progress of reaction was monitored using TLC in 30% ethyl acetate and 70% petroleum ether solvent system. The orange precipitate thus obtained was filtered and washed with cold water to remove the traces of acid or impurities. The obtained product was dried and recrystallized using ethanol.

The other PDTA derivatives were also synthesized using the same procedure.

2.5. *Spectral data*

2.5.1. 4-phenylthiazol-2-amine*:* White solid, Yield: 90%, Melting point: 150-152 °C, IR (KBr, cm^{-1}): 3385, 3245, 3027, 2956, 1700, 1294, 1124, 763; ^{1}H NMR (400 MHz, $CDCl_3$, ppm): δ = 4.08 (s, 2H, N**H**$_2$), δ = 6.76 (s, 1H, C=C**H**-O), δ = 7.40-7.42 (m, 1H, Ar-**H**), δ = 7.48-7.51 (m, 2H, Ar-**H**), δ = 7.76-7.78 (m, 2H, Ar-**H**); ^{13}C NMR (400 MHz, DMSO-d6): δ = 101.74, 125.43, 128.07, 128.66, 129.22, 138.75, 170.17.

2.5.2. 5-(phenyldiazenyl)-4-phenylthiazol-2-amine (H-PDTA): Orange Solid; % Yield = 86%; Melting Point: 193-196 °C; IR (KBr) ν_{max} cm^{-1}: 3373, 3265, 3015, 2953, 1698, 1586, 1438, 1318, 1297, 1210, 1182, 1115, 996, 812, 774; ^{1}H NMR (400 MHz, DMSO-d6, ppm): 7.367-7.503 (m, 3H, Ar**H**), δ = 7.572-7.658 (m, 5H, Ar**H**), δ = 8.028-8.230 (d, J = 9.02 Hz, 2H, Ar**H**), 8.435 (s, 2H, N**H**$_2$); ^{13}C NMR (400 MHz, DMSO-d6, ppm): δ = 121.74, 127.43, 128.07, 128.66, 129.22, 131.57, 133.68, 139.45, 142.58, 151.26, 155.37, 169.18.

2.5.3. 5-(4''-chlorophenyl)diazenyl)-4-phenylthiazol-2-amine (Cl-PDTA): Orange Solid; % Yield = 93%; Melting Point: 235-339 °C; IR (KBr) ν_{max} cm^{-1}: 3394, 3292, 3082, 2929, 1654, 1527, 1481, 1321, 1263, 1203, 1151, 917, 834, 785, 697; ^{1}H NMR (400 MHz, DMSO-d6, ppm): 7.464-7.534 (m, 5H, Ar**H**), δ = 7.618-7.640 (d, J= 8.55 Hz, 2H, Ar**H**), δ = 8.175-8.199 (d, J= 7.66 Hz, 2H, Ar**H**), 8.516 (s, 2H, N**H**$_2$); ^{13}C NMR (400 MHz, DMSO-d6, ppm): δ = 123.25, 128.52, 129.47, 129.83, 130.09, 132.90, 133.50, 139.60, 151.16, 156.36, 170.09.

2.5.4. 5-(4''-methylphenyl)diazenyl)-4-phenylthiazol-2-amine (Me-PDTA): Orange Solid; % Yield = 87%; Melting Point: 200-204 °C; IR (KBr) ν_{max} cm^{-1}: 3464, 3274, 3050, 2927, 1636, 1598, 1487, 1328, 1310, 1265, 1241, 1142, 918, 836; ^{1}H NMR (400 MHz, DMSO-d6, ppm): 2.321 (s, 3H, C**H**$_3$), δ = 7.253-7.273 (d, J= 8.23 Hz, 2H, Ar-**H**), δ = 7.416-7526 (m, 5H, Ar-**H**); δ = 8.163-8.179 (d, J= 7.32 Hz, 2H, Ar-**H**), 8.286 (s, 2H, N**H**$_2$). ^{13}C NMR (400 MHz, DMSO-d6, ppm): δ = 20.97, 121.76, 128.45, 129.49, 129.96, 129.99, 133.79, 139.85, 140.13, 150.52, 154.55, 169.28.

2.5.5. 5-(4''-methoxyphenyl)diazenyl)-4-phenylthiazol-2-amine (OMe-PDTA): Orange Solid; % Yield = 83%; Melting Point: 205-209 °C; IR (KBr) ν_{max} cm^{-1}: 3405, 3298, 3081, 2926, 1648, 1560, 1528, 1483, 1327, 1261, 1212,

1144, 821, 780; ^{1}H NMR (400 MHz, DMSO-d6, ppm): 3.789 (s, 3H, C**H$_3$**), δ = 7.013-7.035 (d, J= 8.83 Hz, 2H, Ar-**H**), δ = 7.401-7.612 (m, 5H, Ar-**H**), δ = 8.159-8.178 (d, J= 9.16 Hz, 2H, Ar-**H**), 8.183 (s, 2H, N**H$_2$**); ^{13}C NMR (400 MHz, DMSO-d6, ppm): δ = 55.55, 114.74, 123.46, 128.45, 129.29, 129.86, 133.92, 139.44, 146.65, 153.36, 160.20, 168.76.

2.5.6. 5-(4''-nitrophenyl)diazenyl)-4-phenylthiazol-2-amine (NO_2-PDTA): Olive Green Solid; % Yield = 91%; Melting Point: 253-257 °C; IR (KBr) ν_{max} cm^{-1}: 3422, 3299, 3068, 2927, 1648, 1526, 1513, 1438, 1364, 1291, 1250, 1193, 1145, 920, 861; ^{1}H NMR (400 MHz, DMSO-d6, ppm): δ = 7.497-7.736 (m, 5H, Ar-**H**), δ = 8.185-8.269 (m, 4H, Ar-**H**), 8.896 (s, 2H, N**H$_2$**); ^{13}C NMR (400 MHz, DMSO-d6, ppm): δ = 122.14, 125.21, 128.68, 130.46, 130.55, 133.21, 145.81 ,156.88, 160.23, 171.85.

2.6. *Theoretical Calculations*

Hyperchem 8.0 software package (HyperChem, 2011) was used to perform all the theoretical calculations reported here. The optimization of the studied PDTA derivatives and quantum mechanics calculations were conducted based on combination of semiemperical Parametric Method 3 (PM3) and molecular mechanics (MM+) calculations. The optimized geometry of H-PDTA is shown in Fig. 1.

2.7. *Kamlet-Taft and Catalán Treatments*

For quantitative assessment of the solute-solvent interactions and their effect on the absorption shifts, multiparameter solvent polarity scale known as linear solvation energy relationship (LSER) proposed by Kamlet, Taft and others (Kamlet *et al.*, 1981; Matanga and Kubata, 1970) has been used. In the most general case, the expression is given by eq.2.

$$\nu = \nu_o + s_{\pi^*}\pi^* + a_\alpha\alpha + b_\beta\beta \quad (2)$$

where $\boldsymbol{\nu_o}$ is the vapor phase wave-number (independent of solvent effects) and $\boldsymbol{\nu}$ are absorption band maxima in a solvent. The coefficients s_{π^*}, a_α and b_β are interpreted as solute properties and indicate the susceptibility of $\boldsymbol{\nu}$ to a change in the corresponding parameter. The coefficient, s_π is related to the solute's polarity/polarizability character, a_α describes its tendency to accept hydrogen bond from the solvent and b_β measures its property to donate hydrogen bond to the solvent. π^*, α and β as a measure of the polarity/polarizability character of the solvent, its hydrogen-bond donor (HBD) and hydrogen-bond acceptor (HBA) capacities, respectively.

Catalán *et al.* (Catalán, 1997; Catalán, 1995) proposed empirical solvent scales: SPP, SA and SB to describe the polarity/polarizability, acidity and basicity of a solvent. The dependence of ν on the SPP, SA and SB parameters is given by eq.3:

$$\nu = \nu_o + s_{SPP}\,SPP + a_{SA}SA + b_{SB}SB \quad (3)$$

The corresponding parameters for different solvents were taken from literature (Kamlet *et al.*, 1983; Catalán, 1997) and are given in Table 2. All least-squares fit analyses were carried out with Microsoft EXCEL 2010 software.

3. Results and Discussion

PDTA derivatives consist of a five membered heterocyclic thiazole ring connected with an azo group (–N=N–) and two phenyl rings (Fig. 1). The absorption spectra of PDTA derivatives were studied in different solvents of varying polarity. The absorption spectra of H-PDTA and NO_2-PDTA are shown in Fig. 2 and their absorption band maxima's (λ_{A1}, λ_{A2}, λ_{A3} and λ_{A4}) are compiled in Table 1.

3.1. *Absorption Spectral Properties*

The absorption spectra of PDTA derivatives is characterized by four bands A1, A2, A3 and A4 in all the solvents located in the UV-vis regions ~255–290 nm and ~411–512 nm, respectively except chloroform (explained later). The overlapped shorter wavelength bands A1 and A2 with λ_{max} ranging from ~255–290 nm are characteristic bands of the phenyl and thiazole rings of the compounds attributed to the π-π^* transitions. While, the longer wavelength band A4 with λ_{max} ranging from ~411–512 nm is the intense one and can be attributed to the π-π^* transition involving the whole molecular structure of the PDTA derivatives (Sidhir *et al*., 2011; Abdalla *et al.*, 2006; Rageh, 2004). Their absorption spectra also show a shoulder peak A3 in the UV-vis region ~280–330 nm, probably due to n-π^* transitions which probably get masked by the more intense π-π^* transitions (Rastogi *et al*., 2011; El-Hendawy *et al*., 2009).

The absorption spectra of PDTA derivatives show bathochromic shift on increasing the solvent polarity from n-hexane to water. It has been found that absorption bands A1, A2 and A4 show bathochromic shifts of ~7–12 nm, 13–18 nm and ~20–50 nm, respectively with increase in solvent polarity. λ_{max} values suggest that the absorption band A4 is most sensitive towards solvent polarity in comparison to other absorption bands A1, A2 and A3.

All derivatives reveal a similar behavior except NO_2-PDTA. The band A3 is clearly visible in the UV region ~310–325 nm unlike other derivatives and can be explained on the basis of extra conjugation due to presence of strong electron withdrawing $–NO_2$ group at para position w.r.t to the –N=N– moiety of NO_2-PDTA. PDTA derivatives show yellowish-orange color on dissolving in all the solvents except NO_2-PDTA which displays a red color. The red color of nitro derivative changes to violet and pink in DMF and DMSO solvents, respectively, while for others the color remain unchanged in these solvents (Fig. 3).

In DMSO along with color change a unique long wavelength peak ~600–650 nm is also observed. This new band can be explained on the basis of the formation of solvated molecular complex of solute (NO_2-PDTA) with DMSO *via* intermolecular hydrogen bonding (Rageh, 2004). Also, the remarkable bathochromic shift in case of polar aprotic solvent DMF and DMSO as compared to other solvents can be ascribed to interaction of PDTA derivatives with the lone pair of electrons present in these solvents (Abdalla *et al.*, 2006; Richmond *et al.*, 1999). The longer wavelength band appears only in DMSO owing to high basicity as well as proton acceptor characteristics of the solvent. The appearance of this band only in the spectra of *p*-NO_2 derivative is due to the strong withdrawing power of the NO_2 group, which decreases the electron density of DMSO molecule (Mahmoud *et al.*, 1987).

PDTA derivatives do not show characteristics color as well as bands A1-A4 in chloroform, instead a single peak near ~311–318 nm is observed (Figs. 2 and 3). This anomalous change can be explained on the basis of photolysis of PDTA derivatives in the chloroform solvent and instead of yellow-orange colored sample a colourless solution is noticed (Figs. 3 & 4) (Hirao and Yonemitsu, 1972).

3.2. *Fluorescence Spectral Properties*

The fluorescence spectra of PDTA derivatives were recorded in a variety of solvents and found to be non-fluorescent. Generally, the non-fluorescent nature of the molecules can be explained on the basis of the following factors: 1) Presence of heavy atom in the molecular structure quenches the fluorescence, 2) Owing to extended structure or higher degree of flexibility of the molecules, excited molecules lose their energies by collision with other molecules or solvent and results in the decrease of fluorescence, 3) When an emission band overlaps with an excitation (absorption) band self-absorption occurs and in this case, emitted photons excite other molecules in the ground state which results in no net emission and 4) due to existence of a low lying n-π^* transition that rapidly converts the excited molecule to the triplet state (intersystem crossing, ISC) and prevent fluorescence (Lakowicz, 2006; Valeur, 2001).

However, in case of PDTA derivatives, due to presence of heteroatom sulphur as substituent, n-π^* transition may be the lowest-lying transition. These transitions enable the excited state molecules to undergo ISC and therefore, render fluorescence.

3.3. *Kamlet-Taft and Catalan Treatments*

The absorption wavelength maxima obtained in various solvents have been analyzed using Kamlet-Taft and Catalan treatment and the results are presented in Table 3. The correlations of the spectroscopic data were quantified by means of multiple linear regression analysis. The absorption frequencies (ν_0) of different PDTA derivatives in vapour phase were calculated using both approaches and are also given in Table 3. The coefficients ν_0, $s_{\pi*}$, b_β, a_α, S_{SPP}, b_{SB} and a_{SA} have confidence intervals at a level of significance of 95%. Among all PDTA derivatives, NO_2-PDTA offer lower ν_0 as a consequence of strong electron withdrawing capacity of nitro group manifested by the lowering of excitation energy.

Using MLRA approaches (eqs. 2 & 3) it was found that b_β, b_{SB}, $s_{\pi*}$ and S_{SPP} coefficients have negative values for all PDTA derivatives (Table 3). The negative values of S_{SPP} and $s_{\pi*}$ indicate an increase in the solvent dipolarity/polarizability. The large negative values of b_β and b_{SB} in ground state reveal the higher HBD ability of the PDTA derivatives, as the amino group participates in the formation of hydrogen bond with the solvents. Large negative values indicate stabilization because hydrogen bonding stabilizes the excited state and decreases the energy gap and a bathochromic shift is observed (Table 3). Large negative values for coefficients, b_β and b_{SB} for NO_2-PDTA are a consequence of the strong electron-withdrawing capacity of $–NO_2$ group. The positive values of a_α and a_{SA} for all PDTA derivatives designate their poor HBA ability except NO_2-PDTA which has negative value of a_{SA} due to eletron-withdrawing nature of $–NO_2$ group (Saha *et al.*, 2008).

3.4. *In Vitro Anti-Oxidant Activities: Correlation With Dipole Moments*

The IC_{50} values were determined using linear trends emerging from $DPPH^{\bullet}$ scavenging ability of PDTA derivatives at different concentrations. Fig. 5 represents their percentage antioxidant activity in ethanol at various concentrations and corresponding IC_{50} values are compiled in Table 4. In the present study, all derivatives except NO_2-PDTA (IC_{50} = 10.709 μg/mL) showed potent $DPPH^{\bullet}$ scavenging activity as that of standard ascorbic acid (IC_{50} = 2.277 μg/mL). NO_2 group (para substituted) being an electron withdrawing interrupts the transfer of an electron to the electrophilic $DPPH^{\bullet}$ and hence, it is justified that NO_2-PDTA is ineffective as an antioxidant (Osman *et al.*, 2012). While, OMe-PDTA exhibit strongest free radical inhibition (IC_{50} = 1.254 μg/mL) in comparison to other derivatives. The presence of stronger electron releasing methoxy group imparts better antiradical capacity to OMe-PDTA.

Fig. 6 represents the free radical scavenging mechanism of $DPPH^{\bullet}$ and concludes that the potent antioxidant activity exhibit by PDTA derivatives is due to presence of free $–NH_2$ group at the heterocyclic thiazole moiety (Devasagayam *et al.*, 2008). Thus, it can be justified that the antioxidant activity is strongly influenced by the structure as well as the substitution of the molecule.

A correlation between $DPPH^{\bullet}$ scavenging activity and dipole moment is also consider to understand the effect of structural and electronic properties of the PDTA derivatives on their antioxidant property. Ground state dipole moments have been calculated theoretically and shown in Table 4. The dipole moment of NO_2-PDTA (μ = 6.642 D) is found to be considerably higher than the other derivatives (Table 3). Because of presence of strong electron withdrawing NO_2 group, the electric dipoles in the excited state are well separated, hence, possess large dipole moments in comparison to other derivatives. For PDTA derivatives, however, a significance trend was noted, molecules with higher dipole moment, show lower $DPPH^{\bullet}$ scavenging value (Rupasinghe *et al.*, 2013). This confirms that molecules with stronger electron releasing groups like methoxy, hydroxyl etc. show potent radical scavenging capacity comparative to electron withdrawing groups ($–NO_2$ group).

3.5. *pH Studies*

The effects of pH on absorption spectra of the PDTA derivatives were studied in aqueous medium in the H_o/pH/H_ range from –5 to 14. The absorption spectra of H-PDTA at different pH values are shown in Fig. 7 and the corresponding data is compiled in Table 5. The protonation and deprotonation phenomena along with possible tautomer species of PDTA derivatives in H_o/pH/H_ range of -5 to 14 are shown in Fig. 8.

H-PDTA show two peaks P1 and P2 in the UV-vis region ~255–290 nm and ~ 420–465 nm, respectively in water. It is clear from the absorption spectral data that the spectral characteristics of H-PDTA in the pH range 2.98–9.10 is due to the neutral species because the data is similar to that obtained in the non-aqueous solvents. The absorption spectra of H-PDTA show the significant displacement in the absorption band maxima of band P2 (λ_{max} shift from 439 nm to 497 nm) on increasing pH up to 14 (Table 5, Fig. 7). This band indicates the formation of a monoanion due to deprotonation from $–NH_2$ moiety and is visible in all the PDTA derivatives (Rastogi *et al.*, 2012).

With decrease in pH i.e. from 2.08 to −1.01 a new blue shifted absorption band P3 with λ_{max} ~390 nm is observed. This band indicates the formation of monocation (MC_1) and corresponds to the protonation of nitrogen atom of thiazole ring. With further decrease in pH, i.e. in going from –2.85 to –5 two new bands P4 and P5 are observed with the absorption band maxima's in the range, ~325 nm and ~550 nm, respectively. The band P4 has lower absorbance while band P5 has larger absorbance in comparison to all other bands. Thus, it can be concluded that these two bands are a result of some tatutomeric species (Huang and Qian *et al.* 2012; Oakes and Gratton, 1998). The observed red shift in band P5 with the increase of acidity up to H_o = –5 suggests the formation of cationic species (MC_2) and corresponds to the protonation of azo group i.e. formation of $–HN^{+}=N–$ moiety (azonium cation) (Tawarah and Abu-Shamleh 1991; Hart and Smyth, 1980). The absorbance band P4 indicates the appearance of small amount of other form due to protonation of free $–NH_2$ group (MC_3) and indicates the formation of NH_3^{+} species (ammonium cation) (Figs. 7 & 8) (Seferoğlu *et al*. 2015, Rajendiran *et al.*, 2010; Berlin, 1972). Thus, it can be concluded that in acidic medium, the protonation results in a tautomeric equilibrium between ammonium (MC_3) and azonium (MC_2) species, which depends prominently on acid concentration as no such band is observed in basic and neutral pH.

A Similar behavior is observed for other PDTA derivatives. Thus two equilibria (Neutral ⇌ Monocation and Neutral ⇌ Monoanion) exist in the ground state for PDTA derivatives along with azonium ↔ ammonium tautomeric equilibrium. Therefore, it is justified that PDTA derivatives show formation of anion in basic medium after pH 12 and monocation formation appears in the pH range 2.08 to –5. It is worthy to mention that the color of

these derivatives changes on changing the medium from acidic to alkaline; which unlocks the possibility for PDTA derivatives as an acid-base indicators.

Results and Discussions

The absorption spectral behavior for PDTA derivatives has been studied in a series of solvents of varying polarity and found to behave differently w.r.t solvent polarity and substituted phenyl moieties. The appearance of longer unique band in DMSO justifies the same (is one such example). The Kamlet-Taft and Catalán results reveal an acceptable correlation with $s\pi^*$, S_{SPP}, b_β, a_α, b_{SB} and a_{SA} parameters with a greater hydrogen bond donating tendency of PDTA derivatives in ground state. The theoretically calculated ground state dipole moment of NO_2-PDTA is considerably higher because of presence of strong electron withdrawing nitro group, and hence, shows poor antioxidant activity comparative to other derivatives. PDTA derivatives are also found to exhibit Neutral ⇌ Monocation and Neutral ⇌ Monoanion equilibriums in highly acidic- and basic mediums, respectively and therefore, can be used as indicator probes in the acid-base titrations.

Table 1
Absorption data of PDTA derivatives.

Solvent[a]	H-PDTA			Cl-PDTA			Me-PDTA			OMe-PDTA			NO_2-PDTA			
	λ_{A1}[b]	λ_{A2}	λ_{A4}	λ_{A1}	λ_{A2}	λ_{A4}	λ_{A1}	λ_{A2}	λ_{A4}	λ_{A1}	λ_{A2}	λ_{A4}	λ_{A1}	λ_{A2}	λ_{A3}[c]	λ_{A4}
n-Hexane	255	271	411	257	274	421	259	274	422	258	270	409	256	260	311	463
Cyclohexane	256	271	412	258	276	421	260	275	424	259	272	411	256	262	314	465
1,4-Dioxane	259	272	422	262	278	434	264	280	446	261	273	427	257	264	315	485
Ethyl acetate	–	273	423	–	280	439	264	276	447	262	274	429	–	266	318	489
Chloroform		316			312			318			314			313		
DCM	259	272	415	260	277	423	265	274	432	260	271	418	255	264	314	474
DMF	–	284	443	–	285	458	–	281	461	–	279	450	–	307	321	510
tert-Butanol	258	268	423	263	280	433	264	273	444	263	272	426	255	266	315	495
DMSO[d]	–	292	449	–	290	462	–	282	465	–	278	456	–	280	323	519
Acetonitrile	255	268	421	261	276	431	264	271	446	259	272	427	256	262	314	485
2-Propanol	257	270	423	262	277	437	265	273	444	262	272	426	258	266	307	486
1-Butanol	259	272	423	263	277	439	265	274	444	261	272	428	259	267	317	490
Ethanol	258	272	421	263	277	438	265	274	445	260	272	430	258	266	315	493
Methanol	259	272	423	263	278	440	265	274	445	260	273	429	258	266	317	493
Ethylene glycol	260	276	427	264	279	443	267	280	451	262	275	434	260	268	318	495
Water	262	278	434	267	281	445	268	282	453	265	277	440	263	272	323	515

[a]Solvents are arranged according to dielectric constants.
[b]$\lambda_{A1,}$ λ_2, λ_{A3} and λ_{A4} indicate the four excitation wavelengths and are expressed in nm.
[c]λ_{A3} is visible in the absorption spectra of NO_2-PDTA. In other derivatives this peak appears as shoulder.
[d]In case of NO_2-PDTA a longest wavelength peak appears at ~628 nm in DMSO.

Table 2

Various solvent parameters used in the Kamlet-Taft and Catalán treatments.

Solvents	Kamlet-Taft parameters			Catalán parameters		
	α	β	π^*	SA	SB	SPP
n-Hexane	0.00	0.00	–0.01	0.000	0.056	0.519
Cyclohexane	0.00	0.00	0.00	0.000	0.073	0.557
1,4-Dioxane	0.00	0.37	0.49	0.000	0.444	0.701
Ethyl acetate	0.00	0.45	0.45	0.000	0.542	0.795
Chloroform	0.44	0.05	0.58	0.047	0.071	0.783
DCM	0.13	0.10	0.73	0.040	0.178	0.876
DMF	0.00	0.69	0.88	0.031	0.613	0.954
tert-Butanol	0.42	0.93	0.41	0.145	0.928	0.829
DMSO	0.00	0.76	1.00	0.072	0.647	1.000
Acetonitrile	0.19	0.40	0.66	0.044	0.286	0.895
2-Propanol	0.76	0.84	0.48	0.283	0.830	0.848
1-Butanol	0.84	0.84	0.47	0.341	0.809	0.837
Ethanol	0.83	0.77	0.54	0.400	0.658	0.853
Methanol	0.98	0.66	0.60	0.605	0.545	0.857
Ethylene glycol	0.90	0.52	0.92	0.717	0.534	0.931
Water	1.17	0.47	1.09	1.062	0.025	0.962

Table 3

Multiparametric correlation of Kamlet-Taft ($\nu = \nu_o + s_{\pi^*}\pi^* + a_\alpha\alpha + b_\beta\beta$) and Catalán ($\nu = \nu_o + s_{SPP}\,SPP + a_{SA}SA + b_{SB}SB$) treatment of PDTA derivatives towards the absorption spectral properties.

Molecule	Kamlet-Taft Parameters					Catalán Parameters				
	ν_o (cm^{-1})	s_{π^*}	a_α	b_β	R^a	ν_o (cm^{-1})	S_{SPP}	a_{SA}	b_{SB}	R^a
H-PDTA	24545	–1285	499	–849	0.906	26233	–3330	223	–117	0.949
Cl-PDTA	23969	–1187	380	–1087	0.899	25556	–2987	7	–464	0.963
Me-PDTA	24122	–1537	424	–1460	0.978	25520	–3432	92	–416	0.985
OMe-PDTA	24644	–1761	583	–836	0.922	26706	–4033	174	–216	0.918
NO_2-PDTA	22023	–1406	68	–1506	0.937	23553	–324	–290	–347	0.931

[a]Correlation coefficients.

Table 4
IC_{50} values of PDTA derivatives and ascorbic acid and their correlation with dipole moments.

Molecules	IC_{50} value (μg/ml)[a]	Dipole moment (D)[b]
Ascorbic Acid	2.277	–
H-PDTA	2.103	1.138
Cl-PDTA	1.606	1.596
Me-PDTA	2.250	1.271
OMe-PDTA	1.254	2.075
NO_2-PDTA	10.709	6.642

[a]DPPH free radical activity.
[b]Calculated theoretically using PM3 method.

Table 5
Absorbance maxima assignment of different prototropic species in H_o/pH/H_ range –5 to 14.

H_o/pH/H_	H-PDTA		Cl-PDTA		Me-PDTA		OMe-PDTA		NO_2-PDTA	
	λ_{P1}-λ_{P5}	AS[a]	λ_{P1}-λ_{P5}	AS	λ_{P1}-λ_{P5}	AS	λ_{P1}-λ_{P5}	AS	λ_{P1}-λ_{P5}	AS
–5.00	271,318,377,556	T	268,328,390,539	T	268,311,399,550	T	270,307,380,545	T	266,350,392,532	T
–2.85	271,321,379,548	T	268,333,390,535	T	267,312,400,545	T	269,309,383,541	T	264,353,395,527	T
–2.06	267,324,389,546	T	265,335,392,532	T	265,314,402,542	T	267,311,390,535	T	262,356,406,524	T
–1.01	266,388,484	MC	265,392,482	MC	263,402,430	MC	266,390,507	MC	260,406,466	MC
–0.33	262,385,484	MC	264,392,482	MC	263,401,430	MC	266,388,504	MC	260,406,466	MC
0.55	261,385,484	MC	264,390,481	MC	263,401,428	MC	265,386,502	MC	260,404,465	MC
1.01	261,386,483	MC	264,390,479	MC	262,400,428	MC	265,386,496	MC	261,403,462	MC
2.08	260,389,483	MC	264,389,480	MC	262,399,426	MC	264,389,496	MC	262,323,519	MC
2.98	260,418	N	264,427	N	262,432	N	264,394	N	262,322,519	N
3.98	260,428	N	264,432	N	262,440	N	264,440	N	262,322,519	N
4.90	261,432	N	264,431	N	263,450	N	264,442	N	263,324,517	N
5.24	262,432	N	263,432	N	263,450	N	264,442	N	262,322,515	N
Water	259,434	N	263,432	N	263,449	N	266,440	N	262,322,515	N
6.90	259,432	N	264,431	N	265,450	N	266,440	N	262,322,517	N
7.98	258,429	N	264,432	N	265,450	N	265,441	N	262,324,517	N
9.10	259,430	N	264,431	N	265,452	N	265,444	N	264,323,517	N
10.04	258,430	N	264,431	N	265,452	N	265,445	N	262,324,518	N
10.92	260,433	N	264,431	N	265,454	N	265,447	N	262,323,518	N
12.00	260,433	N	265,432	N	266,455	N	268,447	N	263,323,529	N
13.00	266,461	MA	265,434	MA	267,460	MA	270,455	MA	265,395,535	MA
14.00	270,497	MA	270,439	MA	272, 493	MA	272,475	MA	265,397,569	MA

[a]Assigned species as N = neutral, MC = monocation, MA = monoanion and T = tautomerism.

(a)

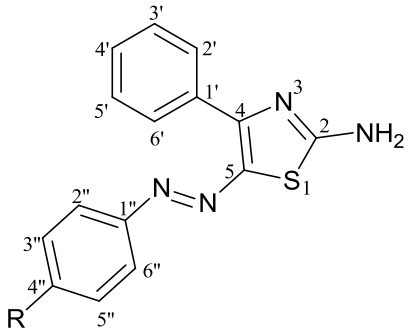

MOLECULES	R =	Abbreviation
5-(phenyldiazenyl)-4-phenylthiazol-2-amine	H	H-PDTA
5-(4"-chlorophenyl)diazenyl)-4-phenylthiazol-2-amine	Cl	Cl-PDTA
5-(4"-methylphenyl)diazenyl)-4-phenylthiazol-2-amine	CH_3	CH_3-PDTA
5-(4"-metoxyphenyl)diazenyl)-4-phenylthiazol-2-amine	OCH_3	OCH_3-PDTA
5-(4"-nitrophenyl)diazenyl)-4-phenylthiazol-2-amine	NO_2	NO_2-PDTA

(b)

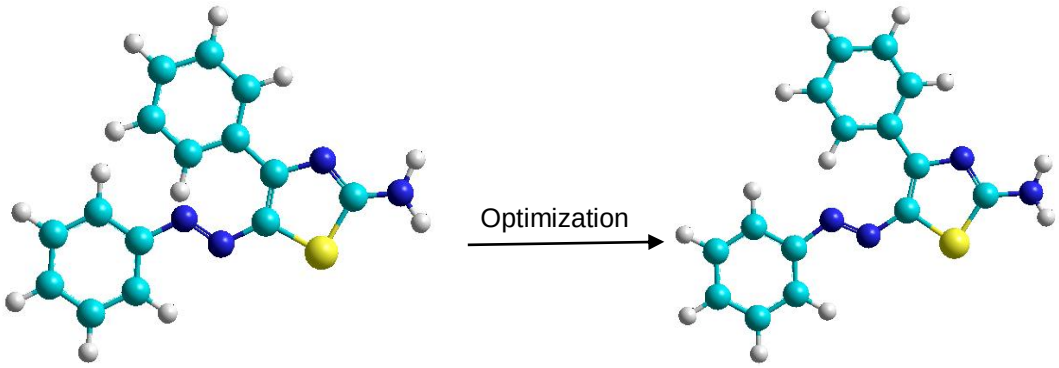

Fig. 1: (a) Structures of 5-(phenyldiazenyl)-4-phenylthiazol-2-amines.
(b) Optimized geometry of H-PDTA in the ground state.

(a)

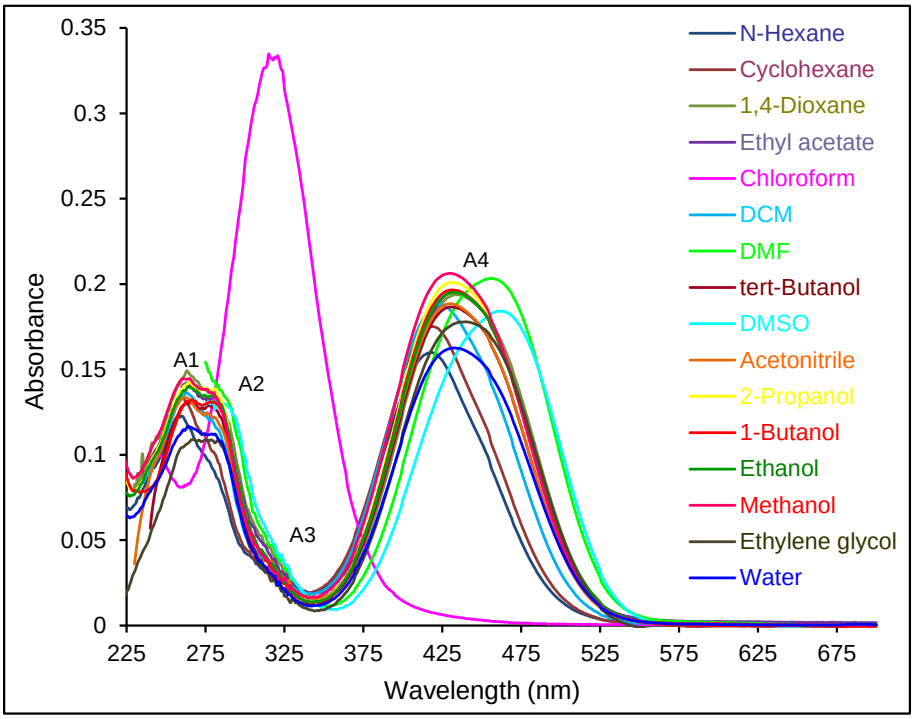

(b)

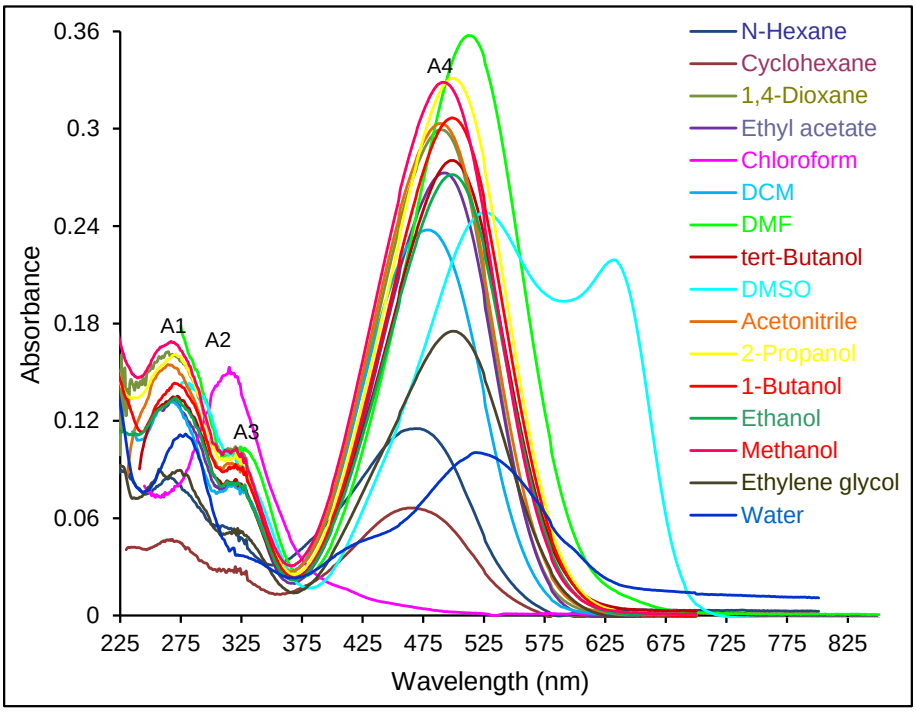

Fig 2: Absorption Spectra of (a) H-PDTA and (b) NO_2-PDTA.

(a)

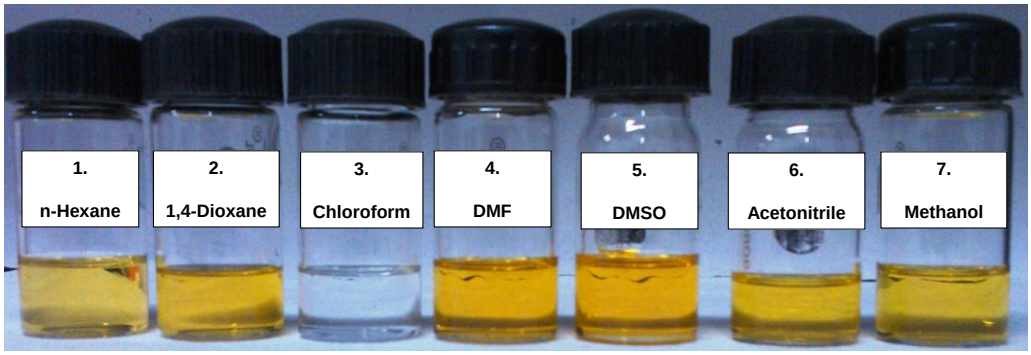

(b)

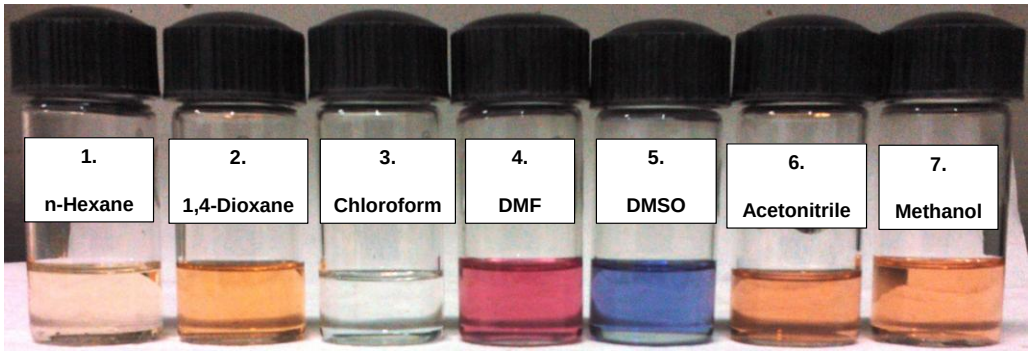

Fig. 3: The appearance of (a) H-PDTA and (b) NO_2-PDTA in different solvents: 1) n-Hexane 2) 1,4-Dioxane 3) Chloroform 4) DMF 5) DMSO 6) Acetonitrile 7) Methanol

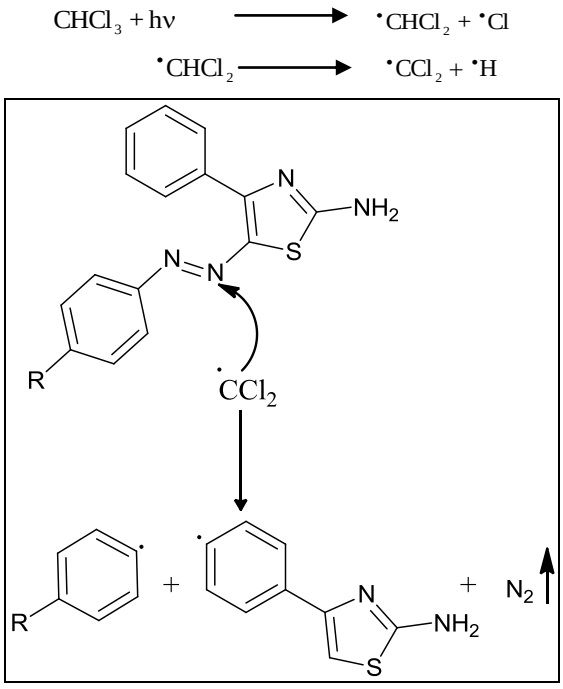

Fig. 4: Dissociation mechanism for PDTA derivatives in chloroform solvent.

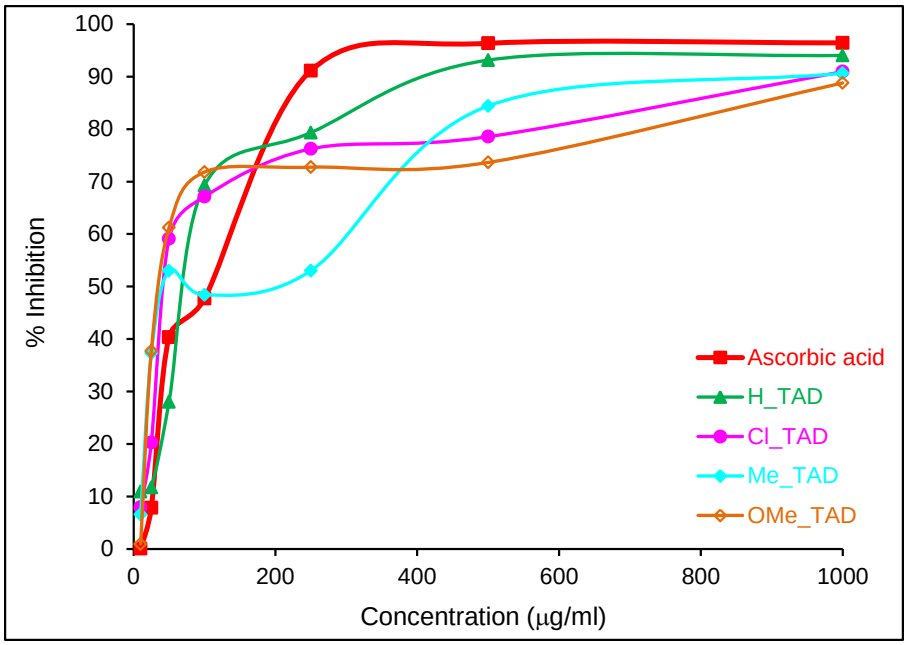

Fig.5: Antioxidant activity of PDTA derivatives by DPPH method in ethanol.

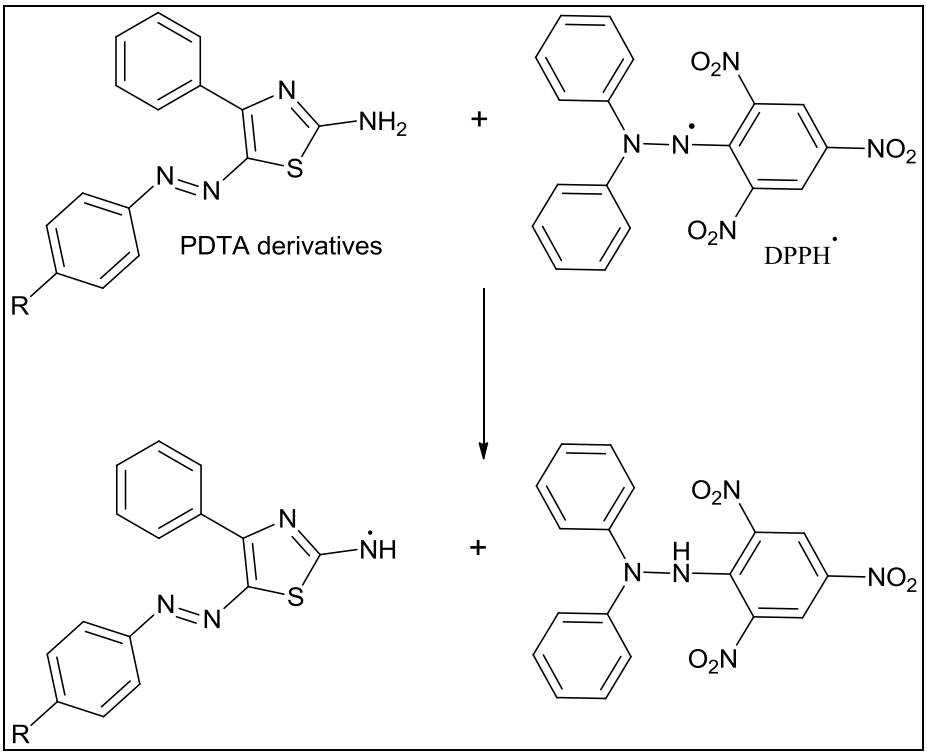

Fig 6: Free radical scavenging mechanism for PDTA derivatives using DPPH.

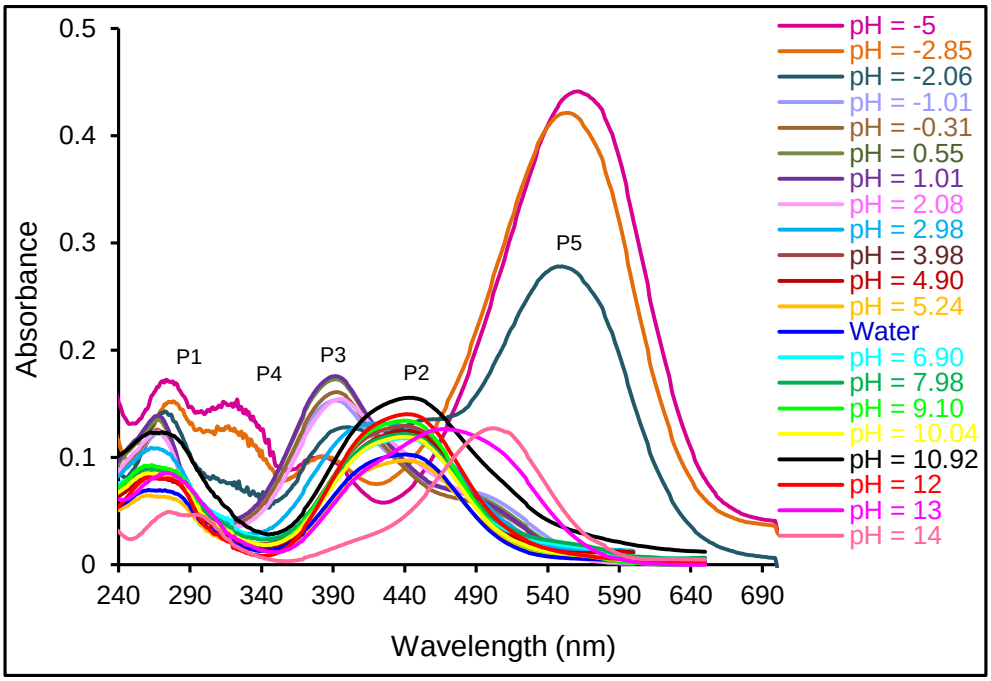

Fig .7: Absorbance spectra of H-PDTA in the H_o/pH/H_ range –5 to 14 in aqueous medium.

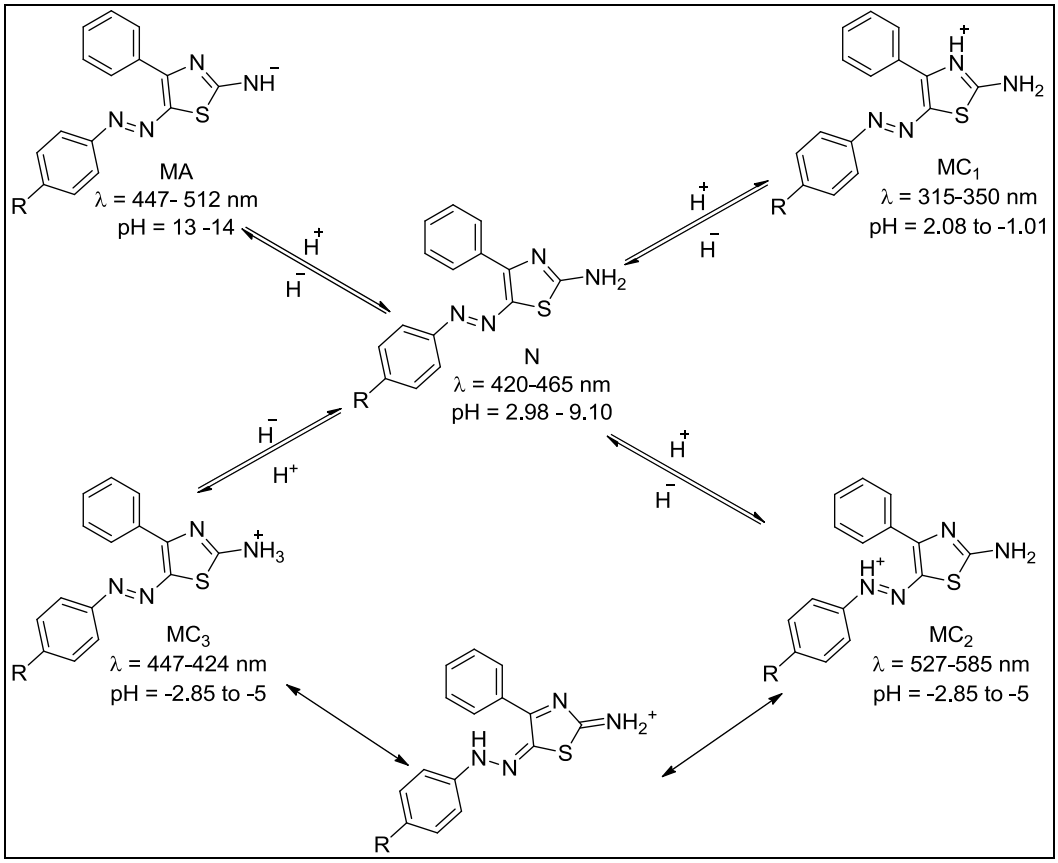

Fig .8: Various prototropic species of PDTAs at different H_o/pH/H_ with their region (R = Ph; N, MC, MA is used for Neutral, Monocation and Monoanion species respectively).

Acknowledgments

Ritu Payal thanks University Grants Commission (UGC), New Delhi for the financial support. The financial support from University of Delhi under the Scheme "To strengthen R & D Doctoral Research Program" is gratefully acknowledged.

References

Geng, J., Dai, Y., Qian, H., Wang, N., Huang, W., 2015. Dyes Pigments 117, 133.

Jia, R., Zheng, C., Yang, D., Sun, J., Wang, H., 2012. Color Technol. 128(4), 290.

Metwally, M.A., Abdel-latifa, E., Amer, F.A., Kaupp, G., 2004. Dyes Pigments 60(3), 249.

Åstrand, P.O., Sommer-Larsen, P., Hvilsted, S., Ramanujam, P.S., Bak, K.L., Sauer, S.P.A, 2000. Chem. Phys. Lett. 325(1-3), 115.

Razus, A.C., Nica, S., Cristian, L., Raicopol, M., Birzan, L., Dragu, A.E., 2011. Dyes Pigments 91(1), 55.

Raposo, M.M.M., Fonseca, A.M.C., Castro, M.C.R., Belsley, M., Cardoso, M.F.S., Carvalho, L.M., Coelho, P.J., 2011. Dyes Pigments 91(1), 62.

Karci, F., Sener, N., Yamac, M., Sener, I., Demircali, A., 2009. Dyes Pigments 80(1), 47.

Saroj, M.K., Sharma, N., Rastogi, R.C., 2012. J. Mol. Struct. 1012, 73.

Sharma, N., Jain, S.K., Rastogi, R.C., 2007. Spectrochim. Acta A 66(1), 171.

Sharma, N., Jain, S.K., Rastogi, R.C., 2003. Bull. Chem. Soc. Jpn. 76(9), 1741.

Kumar, S., Jain, S.K., Rastogi, R.C., 2001. Spectrochim. Acta A 57(2), 291.

Kumar, S., Rao, V.C., Rastogi, R.C., 2001. Spectrochim. Acta A 57(1), 41.

Osman, H., Arshad, A., Lam, C.K., Bagley, M.C., 2012. Chem. Central J. 6, 32.

Hassan, F.A., 2012. Int. J. Appl. Sci. Tech. 2(7), 180.

Ishihara, M., Fujisawa, S., 2007. In Vivo 21, 163.

Scott, G., 1997. Antioxidants in Science, Technology, Medicine and Nutrition, Birmingham, UK.

Beena, Kumar, D., Rawat, D.S., 2012. Bioorg. Med. Chem. Lett. 23, 641.

De, S., Adhikari, S., Tilak-Jain, J., Menon, V.P., Devasagayam, T.P.A., 2008. Chem-Biol Interact. 173, 215.

Ruan, Z.P., Zhang, L.L., Lin, Y.M., 2008. Molecules, 13, 2545.

Paul, M.A., Long, F.A., 1957. Chem. Rev. 57, 1.

Brand-Williams, W., Cuvelier M.E., Berset, C., 1995. LWT - Food Sci. Tech. 28(1), 25.

Bingol, H., Coskun, A., 2011. J. Solution. Chem. 40, 1505.

HyperChem Release 8.0 professional, Hypercube, Inc., USA, 2011.

Kamlet, M.J., Abboud, J.M., Taft, R.W., 1981. Prog. Phys. Org. Chem. 13, 485, Wiley, New York.

Mataga, N., Kubata, T., 1970. Molecular Interactions and Electronic Spectra, Marcel Dekker, New York.

Catalán, J., 1997. J. Org. Chem. 62(23), 8231.

Catalán, J., 1995. J. Org. Chem., 60(25), 8315.

Kamlet, M.J., Abboud, J.L.M., Abraham M.H., Taft, R.W., 1983. J. Org. Chem., 48(17), 2877.

Catalán, J., Díaz, C., 1997. Liebigs Ann. Recueil 9, 1941.

Sidir, Y.G., Sidir I., Berber, H., Tasal, E., 2011. J. Mol. Liquids 162(3), 148.

Amrallah, A.H., Abdalla, N.A., El-Haty, E.Y., 2006. J. Chin. Chem. Soc. 53(3), 697.

Rageh, N.M., 2004. Spectrochim. Acta A 60, 1917.

Saroj, M.K., Sharma, N., Rastogi, R.C., 2011. J. Fluoresc. 21(6), 2213.

Etaiw, S.E.H., Awad, M.K., Fayed, T.A., El-Hendawy, M.M., 2009. J. Mol. Struct. 919(1-3), 12.

Rageh, N.M., 2004. Spectrochim. Acta A 60(1-2), 103.

Allen, H.C., Gragson, D.E., Richmond, G.L., 1999. J. Phys. Chem. B 103(4), 660.

Mahmoud, M.R., Abd El Gaber, A.A., El Roudi, A.M., Soliman, E.M., 1987. Spectrochim Acta A 43(10), 1281.

Hirao, K., Yonemitsu. O., 1972. J.C.S. Chem. Comm. 812.

Lakowicz, J.R., 2006. Principles of fluorescence spectroscopy, 3rd ed. Plenum, New York.

Valeur, B., 2001. Molecular Fluorescence: Principles and Applications, Wiley-VCH Verlag GmbH.

Saha, S.K., Purkayastha, P., Das, A.B., 2008. J. Photochem. Photobiol. A 195(2-3), 368.

Bhullar, K.S., Jha, A., Youssef, D., Rupasinghe H.P.V., 2013. Molecules, 18, 5389.

Chen, X., Tao, T., Wang, Y., Peng, Y., Huang, W., Qian, H., 2012. Dalton Trans. 41, 11107.

Oakes, J., Gratton, P., 1998. J. Chem. Soc., Perkin Trans. 2, 2563.

Tawarah, K.M., Abu-Shamleh, H.M., 1991. Dyes and Pigments 17, 203.

Hart, J.P., Smyth W.F., 1980. Spectrochim. Acta A 36, 279.

Aksungur, T., Arslan, Ö., Seferoğlu, N., Seferoğlu, Z., 2015. J. Mol. Struct. 1099, 543.

Prabhu, A.A.M., Venkatesh, G., Sankaranarayanan, R.K., Siva, S., Rajendiran, N., 2010. Indian J. Chem. A 49, 407.

Barlin, G.B., 1972. J. Chem. Soc. Perkin Trans. 2, 10, 1459.